CRYSTAL GROWTH & DESIGN
2001
VOL. 1, NO. 6
479−484

Crystal Growth of $RbTiOPO_4$:Nb: A New Nonlinear Optical Host for Rare Earth Doping

J. J. Carvajal, R. Solé, Jna. Gavaldà, J. Massons, M. Aguiló, and F. Díaz*

Física i Cristal·lografia de Materials (FICMA), Universitat Rovira i Virgili, Pl. Imperial Tarraco, 1. 43005 Tarragona, Spain

Received June 1, 2001; Revised Manuscript Received September 28, 2001

ABSTRACT: $RbTiOPO_4$ doped with Nb (RTP:Nb) has been revealed as a new nonlinear optical host for rare earth doping. We have studied the growth conditions of single crystals of RTP:Nb doped with Er^{3+} and Yb^{3+} obtained by the TSSG (top-seeded-solution growth)/slow-cooling technique. The concentration of rare earth ions in RTP:Nb was 13 times higher than in RTP crystals. There were significant changes in the morphology of the crystals. While RTP crystals grew with normal morphology, showing the {100}, {201}, {20$\bar{1}$}, {110}, {011}, and {01$\bar{1}$} forms, RTP:Nb crystals show a habit as thin plates, maintaining all the forms above mentioned, but where the {100} form becomes the most developed in the crystal. RTP:Nb,Er and RTP:Nb,Yb crystals show the same habit as RTP:Nb crystals. A noncentric growth system, formed by a stirrer immersed in the growth solution, was used in the crystal growth process to minimize the difference in dimension between the *a*, *b*, and *c* directions in the crystals. We made preliminary optical characterizations of RTP:Nb, such as measuring the transparency window and the refractive indexes. The cutoff wavelength in the UV region shifted to longer wavelengths and the birefringence of the crystals increased when Nb was incorporated into the crystals. Finally, we studied the polarized optical absorption spectra of Er^{3+} and Yb^{3+} in the host at 6K and at room temperature. The samples had a strong dichroism in all three polarizations, which results in significant changes in the intensities of the peaks.

Introduction

$KTiOPO_4$ (KTP) is the best-known member of an important family of compounds whose relevant nonlinear optical properties have made it a widely used crystal in frequency conversion applications such as second-harmonic generation and optical parametric oscillation.[1] KTP and its many isostructural compounds constitute a large field of research. This family of compounds is generalized as $MM'OXO_4$, where M may be K, Na, Rb, Tl, or Cs and, to a lesser extend, Ag and NH_4, or a combination of two of these ions; M′ may be Ti, Ge, V, Zr, Fe, Ga, Nb, Cr, Mn, Mg, or combinations of two of these ions; and X may be P, As, or a combination of the two.[1] As this family has many isomorphous compounds, we can modulate most of its properties. For example, substituting K with Rb reduces the high ionic conductivity of KTP in more than one order of magnitude,[2] or substituting P with As shifts the transmission cutoff edge of the crystals in the IR region to higher wavelengths.[3]

Attempts to dope KTP with rare earth elements (RE^{3+}) have had limited success, because of the low distribution coefficients of these ions in the KTP host. Co-dopants generally increased the distribution coefficient of RE^{3+}. As we have shown in a previous paper,[4] completely substituting K^+ with Rb^+ to form $RbTiOPO_4$ (RTP) clearly improves the distribution coefficient of RE^{3+}. This objective is also achieved using Nb as co-dopant in KTP:RE^{3+}.[5] In both cases, however, the RE^{3+} concentration achieved was still far below those needed for efficient fluorescence from the RE^{3+}'s and, therefore, for practical laser applications. Merging the effect of these two strategies, a concentration of Er^{3+} of 0.65×10^{20} atoms·cm^{-3} has been obtained in a RTP:Nb crystal,[6] which is on the order of the Er^{3+} concentration in other efficient laser materials.

Moreover, the effect of Nb over the nonlinear optical properties of RTP has been studied recently by our group.[6,7] The results indicate a slight enhancement of the generating power of the second harmonic signal for crystals grown in a solution containing around a 2−3 mol % of Nb_2O_5 substituting TiO_2. Furthermore, this efficiency of second harmonic generation observed in RTP:Nb crystals is not reduced when Er^{3+} is present in the crystals by the possible absorption of this ion.

In this paper, we discuss in greater detail the growth conditions of RTP:Nb, RTP:Nb:Er, and RTP:Nb:Yb single crystals of suitable size and quality for later characterizations. We have included some of these characterizations, e.g., refractive indexes measurements of the host and optical absorption properties of Er^{3+} and Yb^{3+} in this matrix.

Experimental Section

Crystal Growth. RTP crystallizes in the orthorhombic system, spatial group of symmetry $Pna2_1$, and cell parameters $a = 12.974(2)$ Å, $b = 6.494(3)$ Å, and $c = 10.564(6)$ Å, $Z = 8$.[8] RTP melts incongruently in air around 1443 K,[9] so they cannot be obtained directly from the melt. RTP has traditionally been grown by high-temperature flux methods. In this study, we used the TSSG (top-seeded-solution growth) method in combination with a slow-cooling process.

We grew single crystals of RTP, RTP:Nb, RTP:Nb:Er, and RTP:Nb:Yb of suitable size and quality for optical investigation. The experiments were carried out in a vertical cylindrical furnace constructed by ourselves using Kanthal AF resistance heating wire of 1 mm in diameter, rolled on a 50 cm in length alumina cylinder of 9 cm in diameter. The furnace had a single zone with a useful thermic area of 30 cm in length and 7.5 cm in diameter. All this system was insulated thermically by

* To whom correspondence should be addressed. E-mail: diaz@quimica.urv.es.

10.1021/cg015528+ CCC: $20.00
Published on Web 10/16/2001

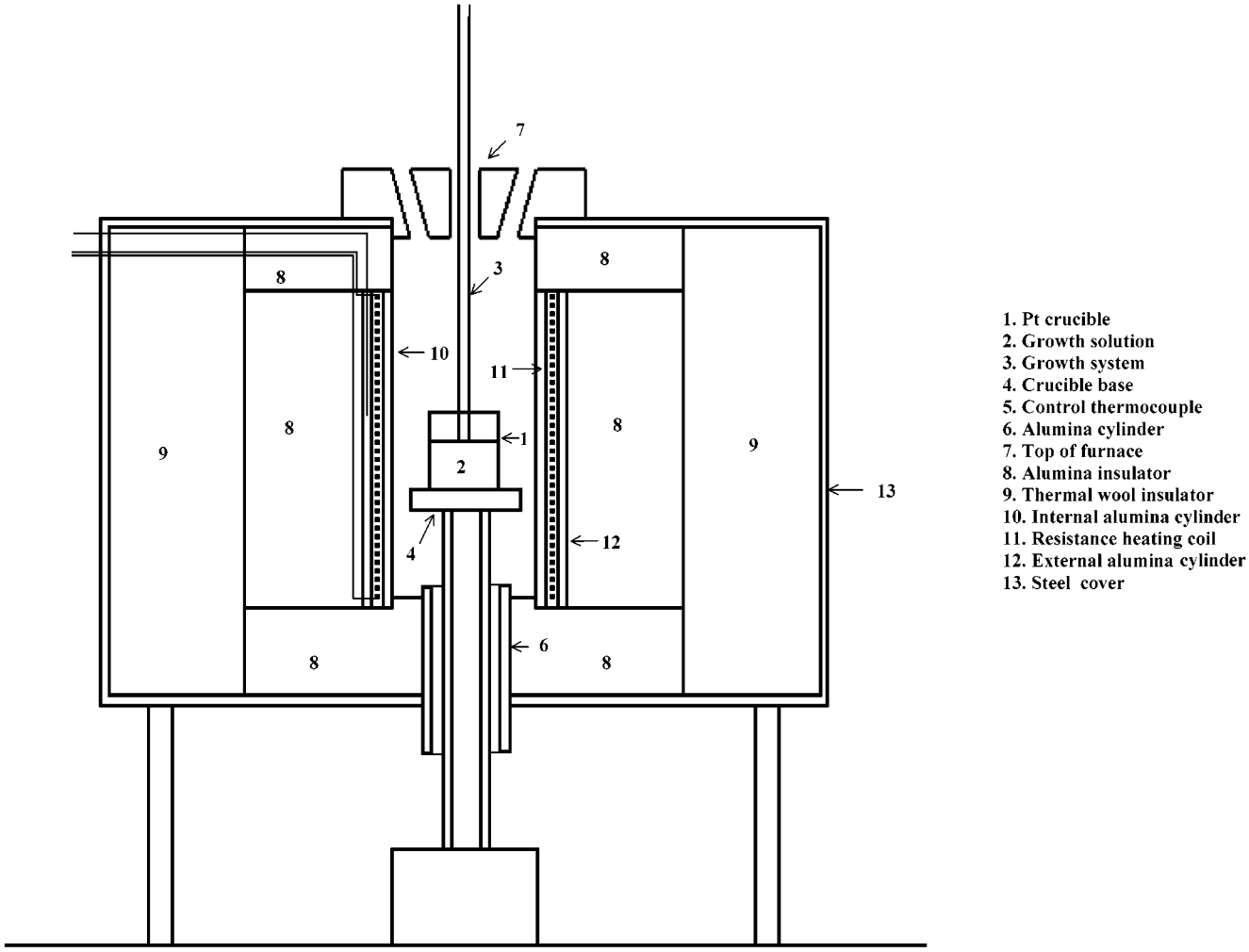

Figure 1. Schematic view of the crystal growth furnace used in this work.

Table 1. Growth Data Associated with Nb Doped and Nb, Er, or Nb, Yb Codoped RTP Single Crystals[a]

A	B	C	D	E	F	G	H	I	J	K
	42.9−35.1−22−0−0−0	*c*	1180	3 K/0.1 K·h^{-1}	10.0 × 9.0 × 10.0	1.183				$RbTiOPO_4$
				7 K/0.05 K·h^{-1}	5.3 × 5.5 × 7.5	0.278				
Nb	42.9−35.1−21.6−0.4−0−0	*c*	1195	3 K/0.1 K·h^{-1}	2.7 × 7.3 × 4.5	0.200	0.56			$RbTi_{0.98}Nb_{0.02}OPO_4$
				10 K/0.05 K·h^{-1}	3.3 × 7.4 × 6.1	0.294				
Nb	42.9−35.1−20.7−1.3−0−0	*c*	1199	3 K/0.1 K·h^{-1}	3.2 × 5.8 × 5.5	0.184	0.49			$RbTi_{0.94}Nb_{0.06}OPO_4$
				10 K/0.05 K·h^{-1}	3.6 × 5.4 × 5.4	0.184				
Nb,Er	42.9−35.1−20.9−0.7−0.4−0	*c*	1173	12 K/0.1 K·h^{-1}	2.1 × 5.5 × 5.2	0.147	0.57	0.04		$RbTi_{0.966}Nb_{0.032}Er_{0.002}OPO_4$
					2.2 × 5.0 × 4.5	0.113				
Nb,Yb	42.9−35.1−20.2−1.3−0−0.4	*c*	1186	5 K/0.1 K·h^{-1}	3.6 × 6.3 × 6.6	0.253	0.63		0.35	$RbTi_{0.91}Nb_{0.08}Yb_{0.01}OPO_4$
				5 K/0.05 K·h^{-1}	1.6 × 5.0 × 4.3	0.071				
				5 K/0.02 K·h^{-1}						

[a] A: doping ions. B: solution composition ($Rb_2O-P_2O_5-TiO_2-Nb_2O_5-Er_2O_3-Yb_2O_3$). C: seed crystallographic orientation. D: saturation temperature (K). E: cooling program: decreased temperature interval/rate of decreasing of temperature. F: crystal dimensions in *a*, *b*, and *c* crystallographic directions, respectively (mm^3). G: crystal weight (g). H: K_{Nb}. I: K_{Er}. J: K_{Yb}. K: stoichiometry.

thermal wool and an external cover of steel. A schematic view of this furnace can be seen in Figure 1. The furnace was controlled by a Eurotherm 818P controller/programmer. The solutions were prepared by mixing the appropriate amounts of Rb_2CO_3 (99%), $NH_4H_2PO_4$ (99%), TiO_2 (99.9%), Nb_2O_5 (99.9%), Er_2O_3 (99.99%), and Yb_2O_3 (99.99%), which we used as starting materials, to obtain the compositions listed in Table 1. We used cylindrical platinum crucibles of 125 cm^3, 6.5 cm in height, and 5.0 cm in diameter, filled with solutions weighing about 160 g. The axial gradient of temperature in the solution was of 1.3 K·cm^{-1} at the first centimeter and 0.8 K·cm^{-1} at the next 1.5 cm, being hotter on the bottom than on the surface of the solution. The radial gradient was constant, and its value was 1.8 K·cm^{-1}. Then, the zone where crystals were grown have a low-temperature gradient. The temperature was kept at 50−100 K above the expected saturation temperature for 3−5 h to homogenize the solution. RTP crystals were grown on RTP seeds, whereas the rest of the crystals were grown on RTP:Nb seeds. Both RTP and RTP:Nb seeds were oriented with the *c* crystallographic direction normal to the surface of the solution and fixed to a growth device comprising a stirrer immersed in the growth solution and two seeds symmetrically distributed about 1.5 cm from the rotation axis and at 2 cm from the platinum turbine, that acts as stirrer, in contact with the surface of the solution (see our previous study[6]). This system increases the stirring of the solution and favors mass transport conditions. The *a* crystallographic direction of the seeds was always placed in the radial direction of the rotation movement. The saturation temperature was determined by observing the dissolution or growth

of the two seeds in contact with the surface of the solution. The growth process was carried out by decreasing the temperature of the conditions outlined in Table 1. The velocity of rotation was constant in all experiments (65 rpm). When the thermal ramp of growth was finished, we removed the crystals slowly from the solution to minimize thermal stress and decreased the temperature of the furnace to room temperature at a rate of 15 $K \cdot h^{-1}$.

Dopant Concentrations. The dopant concentration in the crystals was measured by electron probe microanalysis (EPMA). A Cameca CAMEBAX SX-50 was used in wavelength dispersive mode operating at 25 kV accelerating voltage and 30 nA beam current for Nb and 100 nA for Er. A pure RTP crystal, grown by ourselves, was used as a standard for Rb, Ti, P, and O. This crystal was used as a standard to minimize the matrix effects in the samples because of its similar chemical composition. $LiNbO_3$, provided by C. M. Taylor, was used as a standard for Nb; REE1, a synthetic glass with a base of Si−Al−Ca and an Er concentration of 4.09% in weight manufactured by P&H Developments, was used for Er; and YbF_3, developed by Micro-Analysis Consultants Ltd., was used for Yb.

Optical Characterization. Refractive indexes were measured in $RbTiOPO_4$ and $RbTi_{0.94}Nb_{0.06}OPO_4$ crystals by the minimum deviation angle using prisms at 1.064 and 0.532 μm.[10] The refractive indexes were measured with a BMI SAGA seeded Nd:YAG laser.

Transmission and absorption studies were made on RTP and RTP:Nb crystals with a Varian Cary 500 Scan spectrophotometer in the 300−3000 nm region, and with an FTIR Midac Prospect spectrophotometer in the 3000−10000 nm region. The optical absorption bands of Er and Yb in this matrix were studied at room temperature and 6 K using a Leybold close circuit cryostat. The measurements were made by polarizing the incident beam parallel to each crystallographic axis in the sample.

Results and Discussion

Crystal Growth. Table 1 shows the crystal growth conditions and the results of the experiments made. There were some differences in the results with growth experiments of RTP:Nb crystals with respect to pure RTP crystals. RTP and RTP:Nb crystals grew with the {100}, {201}, {20$\bar{1}$}, {110}, {011}, and {01$\bar{1}$} forms, but RTP:Nb crystals have the {100} more developed showing a thin plate habit (Figure 2).

It is well-known that changes in morphology of crystals grown in doped solutions can be caused by poisoning of the growth sites on the crystal by the attachment of the dopant species. In fact, we have observed that the presence of Nb_2O_5 in the solution, even at low concentrations, affects the morphology of the crystals.

However, we have observed that by improving the mass transport conditions in the solution, the crystals grew with higher quality and the differences of dimension between the *a*, *b*, and *c* directions decreases. In highly viscous solutions, as is the case of the growth solution of RTP crystals, the drop in temperature leads to a high level of supersaturation in some areas of unstirred growth solutions. In these areas, crystals grow quickly, overall in the direction with a higher velocity of growth. Stirring the solution improves the mass transport efficiency and minimize problems associated with nonhomogeneous supersaturation. Stirring the solution also resulted in a decrease in the occurrence of spontaneous nucleation during the growth process.

Another problem associated with the increase of concentration of Nb_2O_5 in the solution were cracks appearing from the crystal seed. This problem could be

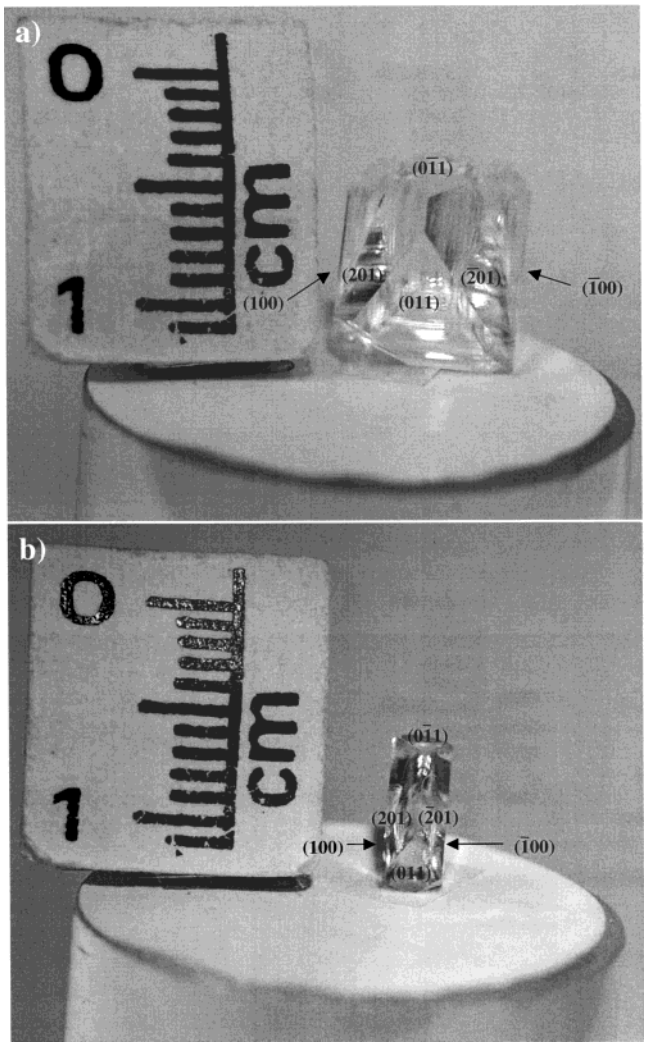

Figure 2. (a) $RbTiOPO_4$ and (b) $RbTi_{0.94}Nb_{0.06}OPO_4$ crystals grown in *c* oriented seeds.

associated with the mismatch between the cell parameters of RTP and these ones of RTP:Nb. In growth experiments of KTP:Nb crystals, a similar problem was observed,[11] but using KTP:Nb seeds solves this problem to a large extent. From our comparative studies with RTP and RTP:Nb seeds, we have concluded that the cracks in the crystal appeared less often with RTP:Nb seeds than with RTP seeds, but at this stage they could not be fully avoided.

Our results indicate that the presence of Nb_2O_5 in the solution strongly influences the growth of RTP crystals. A more detailed study of the positions of Nb in the crystal lattice is required to better understand the changes in the growth mechanisms.

The saturation temperature of these crystals increases as the concentration of Nb_2O_5 increases in the growth solution. But this saturation temperature decreases when the rare earth ions are present in the solution. When the concentration of Nb_2O_5 in the solution increases, the weight of the crystals decreases, using the same growth conditions, due to a decreasing of the rate of growth. Our results seem to indicate that the velocity of growth in the *b* and *c* directions in RTP: Nb, RTP:Nb:Er, and RTP:Nb:Yb crystals become similar, as can be seen in Table 1.

Table 2. Principal Refractive Indexes of $RbTiOPO_4$ and $RbTi_{0.94}Nb_{0.06}OPO_4$ Crystals Determined in This Work

		$RbTiOPO_4$	$RbTi_{0.94}Nb_{0.06}OPO_4$
0.532 μm	n_x	1.8128	1.8187
	n_y	1.8215	1.8554
	n_z	1.9195	1.9422
1.064 μm	n_x	1.7712	1.7772
	n_y	1.7775	1.8067
	n_z	1.8580	1.8727

Dopant Concentration. The concentrations of Nb, Er, and Yb in these samples where analyzed by EPMA. The most significant result obtained was that the concentration of Er in RTP:Nb crystals was 13 times higher than that previously obtained in RTP:Er crystals.[4] The concentration of Er achieved in RTP:Nb:Er crystals was $[Er^{3+}] = 0.65 \times 10^{20}$ ions·cm^{-3}, whereas in RTP:Er crystals the concentration achieved was $[Er^{3+}] = 0.05 \times 10^{20}$ ions·cm^{-3}.

The distribution coefficients of Nb, Er, and Yb were calculated from their concentration in the crystals and in the solution, according to the expression, $K_x = \{[X]/([Ti] + [Nb] + [RE])\}_{crystal}/\{[X]/([Ti] + [Nb] + [RE])\}_{solution}$ where X = Nb, Er, or Yb, and RE = Er or Yb. The distribution coefficients of Nb and Er or Yb for each crystal experiment are shown in Table 1.

When we increased the concentration of Nb in the solution, the distribution coefficient of Nb in the crystal decreases. This effect could be easily explained in terms of the saturation effect of dopant in the crystal.

The distribution coefficients of Nb in these samples were clearly greater than those of the rare earth ions. To explain this behavior, we suppose that Nb in RTP crystals substitutes Ti in the crystal lattice, as it was observed in KTP.[12] The ionic radius of Nb^{5+} in an octahedrical environment is 0.680 Å, which is much closer to that of Ti^{4+} (0.670 Å) than it is the ionic radii of Er^{3+} (0.890 Å) or Yb^{3+} (0.868 Å).[13]

Refractive Indexes Measurements. Accurate measurements of the refractive indexes of a nonlinear optical material are needed to accurately predict the expected phase-matching angle and the angular and spectral bandwidth acceptances. Table 2 shows the values of the principal refractive indexes of $RbTiOPO_4$ and $RbTi_{0.94}Nb_{0.06}OPO_4$ at 0.532 and 1.064 μm. As we can see, the refractive indexes of RTP:Nb were significantly different from those of pure RTP. Whereas n_x practically did not change, n_y and n_z increased substantially. This implies an increase in birefringence as with KTP:Nb crystals.[14]

Optical Absorption of RTP:Nb. We studied the optical transmission window and optical absorption properties of RTP and RTP:Nb. Figure 3 shows the optical transmission spectra of an $RbTi_{0.94}Nb_{0.06}OPO_4$ crystal. We found changes in the cutoff wavelength in the UV region when Nb was present in the crystals. The cutoff wavelength in this region shifted significantly to longer wavelengths, e.g., from 342 to 350 nm in spectra taken with polarized light parallel to the *c* crystallographic direction in RTP and RTP:Nb crystals, respectively. The cutoff wavelength was defined by its value when the absorption coefficient (α) decays by e. This shifting was clearer when we studied α rather than the transmission: α decreased more gently in the sample with Nb at wavelengths shorter than 400 nm (see Figure 3), but at longer wavelengths, was similar for RTP and RTP:Nb crystals.

Optical Absorption of RE Ions. Er^{3+} and Yb^{3+} doping has been extensively studied in many matrixes to obtain laser radiation around 1.5 μm[15] and 1 μm,[16−18] respectively.

There is interest in Er^{3+} for applications in optical communications at long distances. This is because of its efficient emission near the region of optical losses in silica fibers (1.5 μm) attributed to the $^4I_{13/2} \rightarrow {}^4I_{15/2}$ transition.[19,20] In medicine, one interesting application is the $^4I_{11/2} \rightarrow {}^4I_{13/2}$ transition, which emits around 2.8 μm.[20]

The optical absorption of Er^{3+} in single crystals is characterized by $^{2S+1}L_J$ multiplets, whose degeneracy is partially lifted by the crystal field that produces Stark sublevels. Figure 4 shows the polarized absorption spectra of Er^{3+} in an RTP:Nb crystal at room temperature and 6 K. The erbium concentration of this crystal was 0.65×10^{20} ions·cm^{-3}. The crystal was previously annealed at 773 K for 3 h to prevent the appearance of broad absorption bands similar to that observed in reduced KTP samples[21] and in KTP:W samples.[22] Although we have not made any specific studies to identify the origin of these absorption bands, we can assume that are caused by redox processes by analogy of these bands observed in KTP.[21,22] The residual background was analytically evaluated in the side region of each multiplet and discounted from the spectra measured. In these RTP:Nb:Er crystals, eleven multiplets, namely, $^4G_{9/2}$, $^4G_{11/2}$, $^2H_{9/2}$, $^4F_{3/2}$, $^4F_{5/2}$, $^4F_{7/2}$, $^2H_{11/2}$, $^4S_{3/2}$, $^4F_{9/2}$, $^4I_{11/2}$, and $^4I_{13/2}$ were clearly resolved. The $^2K_{15/2}$ and $^4I_{9/2}$ manifolds, were identified but could not be resolved because of their low intensity. The manifolds presented in these figures were the most representative ones in the matrix. The $^4I_{13/2}$ manifold had an important magnetic dipole component, whereas $^2H_{11/2}$ was due to pure electric dipole transitions. The intensities of these spectra were higher than the intensities of the spectra of RTP:Er crystals,[4] which shows that the concentration of Er^{3+} was higher when Nb was used as codopant. Another important aspect is the strong dichroism of this sample. The intensities of the spectra collected with the incident polarized light parallel to the *c* direction were, generally, slightly higher than in the spectra collected using incident polarized light parallel to the *b* direction. However, the absorption coefficient generally dropped considerably in spectra collected with incident polarized light parallel to the *a* direction. In the $^2H_{11/2}$ manifold, this behavior was not followed at room temperature, and some of the most intense peaks of this manifold, collected using incident polarized light parallel to the *b* direction, exceeded in intensity the corresponding ones collected with incident polarized light parallel to the *c* direction. The $^4I_{13/2}$ manifold had another different behavior: the intensities of all the peaks in the three polarization studies at 6 K were so similar that it was difficult to distinguish one from the other.

Yb^{3+} has only two optically accessible 4f electronic states: the $^2F_{7/2}$ ground state, and the $^2F_{5/2}$ excited state. The difference in energy is around 10 000 cm^{-1}, and the states are split by the crystal field. This energy fits the emission from diode and quantum-well lasers quite well. The ytterbium-doped lasers are also characterized by a

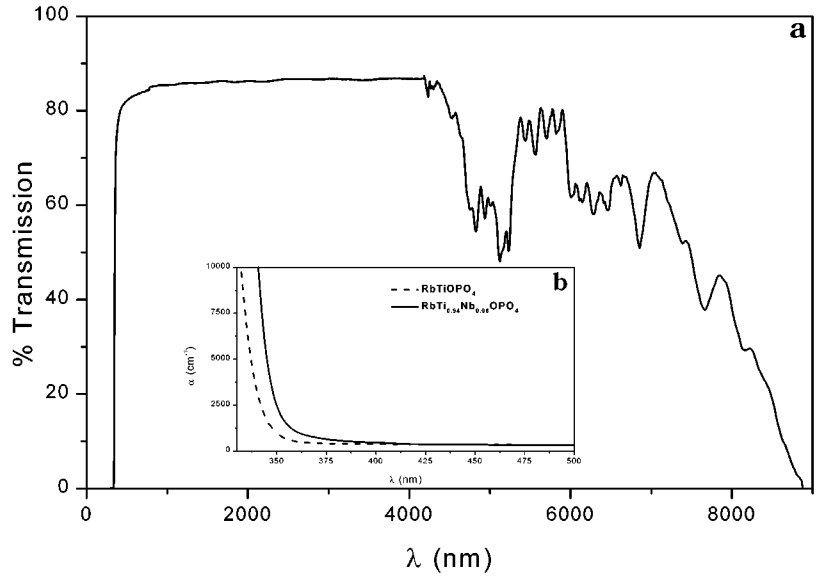

Figure 3. (a) Transparency window of $RbTi_{0.94}Nb_{0.06}OPO_4$ crystal and (b) evolution of the cutoff wavelength in the UV region with the concentration of Nb.

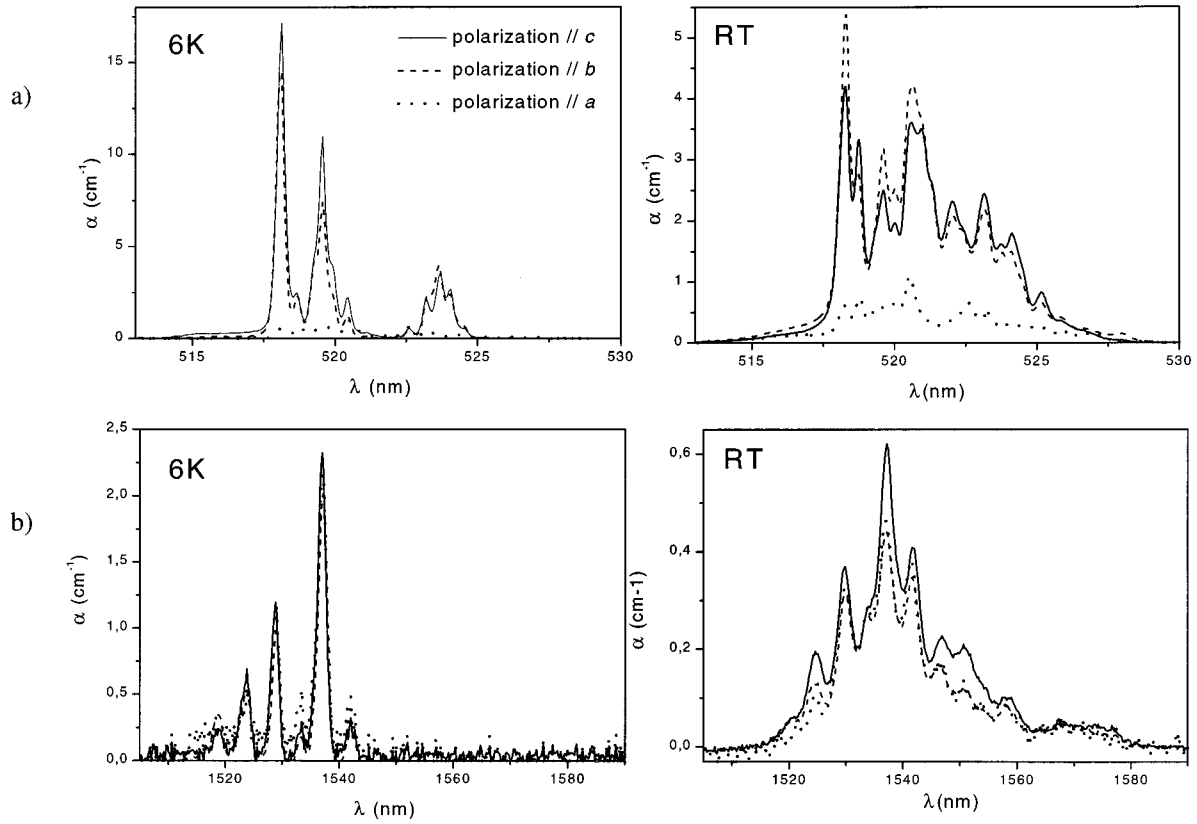

Figure 4. Polarized optical absorption spectra of Er^{3+} in RTP:Nb crystal at 6 K and room temperature (RT): (a) $^2H_{11/2}$ and (b) $^4I_{13/2}$ manifolds.

substantial long radiative lifetime, which improves pumping efficiency. The reduced quantum defect between absorption and emission also reduces the heat generated in the laser crystal, which increases the efficiency of the laser and improves prospects for power scaling.[23]

We also studied the optical absorption spectra of Yb^{3+} in this matrix at room temperature in the three polarizations (incident polarized light parallel to the *a*, *b*, and *c* axes), as can be seen in Figure 5. The only contribution from Yb^{3+} was in the 800−1100 nm range; this was attributed to the $^2F_{5/2}$ manifold. Again, a strong dichroism was observed, but this was different from the dichroism with Er^{3+}. Although the three peaks in this manifold were observed in the three polarized spectra, the intensities of these peaks depended on the polarization. Figure 5 shows that the intensities of the two external peaks of the spectrum parallel to the *c* direction and the intensities of the external peaks of the spectrum parallel to the *b* direction were inversed. For the

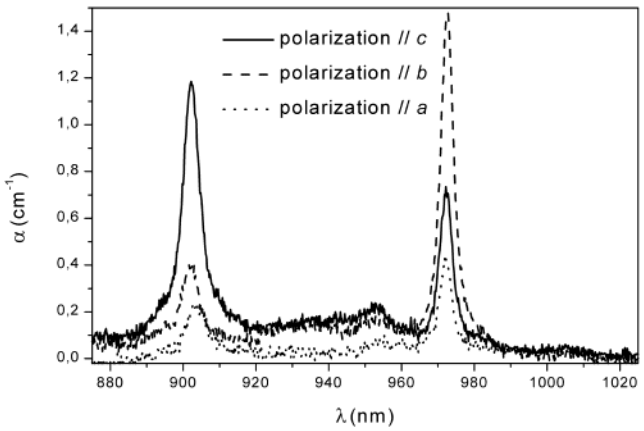

Figure 5. Polarized optical absorption spectra of Yb^{3+} in RTP: Nb crystals at room temperature.

spectrum parallel to the *c* direction, the most intense peak was around 900 nm and for the spectrum parallel to the *b* direction the most intense peak was around 971 nm. The spectrum collected parallel to the *a* direction was less intense than the others. Although this spectrum behaved like the spectrum parallel to the *b* direction, the difference between the intensities of the two external peaks of this manifold was not so great. Finally, in all spectra, the intensity of the internal peak, located around 952 nm, was so low that it was difficult to identify.

Conclusions

We have successfully grown RTP:Nb:Er and RTP:Nb:Yb crystals by the TSSG/slow-cooling technique. The concentrations of Er and Yb in these crystals, as determined by EPMA, were higher than in crystals grown without Nb doping. These results agree with the optical absorption spectra of the rare earth ions, which are more intense than those of RTP:Er crystals. This indicates that the rare earth concentration could be high enough to obtain efficient luminescence from the rare earth ion. All these results open the possibility of obtaining a new self-doubling material. The optical characterization of this new host shows that RTP:Nb refractive indexes are higher than those of RTP, and that the birefringence of the crystals is higher. Finally, the cutoff wavelength of the transmission window in the UV region shifted to longer wavelengths than with pure RTP.

Acknowledgment. This work has been supported by CICyT under projects MAT99-1077-C02 and 2FD97-0912-C02 and by CIRIT under project 1999SGR 00183. J.J. Carvajal would also like to acknowledge the grant from the Catalonian Government (2000FI 00633 URV APTIND). Our group also thanks Dr. X. Llovet from Universitat de Barcelona for useful help in problems related with EPMA measurements.

References

(1) Hagerman, M. E.; Poeppelmeir, K. R. *Chem. Mater.* **1995**, *7*, 602.
(2) Voronkova, V. I.; Yanovskii, V. K. *Izvestiya Akad. Nauk SSSR Org. Mater.* **1988**, *24*, 273.
(3) Hansson, G.; Karlsson, H.; Wang, S.; Laurell, F. *Appl. Optics* **2000**, *39*, 5058.
(4) Rico, M.; Zaldo, C.; Massons, J.; Díaz, F. *J. Phys. Condens. Matter.* **1998**, *10*, 10101.
(5) Solé, R.; Nikolov, V.; Koseva, I.; Peshev, P.; Ruiz, X.; Zaldo, C.; Martín, M. J.; Aguiló, M.; Díaz, F. *Chem. Mater.* **1997**, *9*, 2745.
(6) Carvajal, J. J.; Nikolov, V.; Solé, R.; Gavaldà, Jna.; Massons, J.; Rico, M.; Zaldo, C.; Aguiló, M.; Díaz, F. *Chem. Mater.* **2000**, *12*, 3171.
(7) Carvajal, J. J.; Solé, R.; Gavaldà, Jna.; Massons, J.; Rico, M.; Zaldo, C.; Aguiló, M.; Díaz, F. *J. Alloys Compd.* **2001**, *323−324*, 231.
(8) Thomas, P. A.; Mayo, S. C.; Watts, B. E. *Acta Crystallogr.* **1992**, *B48*, 401.
(9) Cheng, L. K.; Bierlein, J. D.; Ballman, A. A. *J. Cryst. Growth* **1991**, *110*, 697.
(10) Física i Cristal·lografia de Materials, unpublished material.
(11) Wang, J.; Liu, Y.; Wei, J.; Jiang, M.; Shao, Z.; Liu, W.; Jiang, S. *Cryst. Res. Technol.* **1997**, *32*, 319.
(12) Thomas, P. A.; Watts, B. E. *Solid State Commun.* **1990**, *73*, 97.
(13) Shannon, R. D. *Acta Crystallogr.* **1976**, *A32*, 751.
(14) Cheng, L. T.; Cheng, L. K.; Harlow, R. L.; Bierlein, J. D. *Appl. Phys. Lett.* **1994**, *64*, 155.
(15) Van den Hoven, G. N.; Van der Elsken, J. A.; Polman, A.; Van Dam, C.; Van Uffelen, K. W. M.; Smit, M. K. *Appl. Optics* **1997**, *36*, 3338.
(16) Montoya, E.; Sanz-García, J. A.; Bausá, L. E. *Spectrochim. Acta Part A* **1998**, *54*, 2081.
(17) Montoya, E.; Lorenzo, A.; Bausá, L. E. *J. Phys.: Condens. Matter.* **1999**, *11*, 311.
(18) Métrat, G.; Boudeulle, M.; Muhlstein, N.; Brenier, A.; Boulon, G. *J. Cryst. Growth* **1999**, *197*, 883.
(19) Dominiak-Dzik, G.; Golab, S.; Pracka, I.; Ryba-Romanowski, W. *Appl. Phys. A* **1994**, *58*, 551.
(20) Pujol, M. C.; Rico, M.; Zaldo, C.; Solé, R.; Nikolov, V.; Solans, X.; Aguiló, M.; Díaz, F. *Appl. Phys. B* **1999**, *68*, 187.
(21) Martín, M. J.; Bravo, D.; Solé, R.; Díaz, F.; López, F. J.; Zaldo, C. *J. Appl. Phys.* **1994**, *76*, 7510.
(22) Martín, M. J.; Zaldo, C.; Díaz, F.; Solé, R.; Bravo, D.; López, F. J. *Radiat. Eff. Defects Solids* **1995**, *136*, 243.
(23) Wang, P.; Dawes, J. M.; Deckker, P.; Knowles, D. S.; Piper, J. A. *J. Opt. Soc. Am. B* **1999**, *16*, 63.

CG015528+